Crystal Structure of the Anthrax Drug Target, *Bacillus anthracis* Dihydrofolate Reductase†

Brad C. Bennett,‡ Hai Xu,‡ Richard F. Simmerman,‡ Richard E. Lee,§ and Chris G. Dealwis*,‡

Department of Biochemistry, Cellular & Molecular Biology, University of Tennessee, Knoxville, Tennessee 37996, and Department of Pharmaceutical Sciences, University of Tennessee Health Sciences Center, Memphis, Tennessee 38163

Received March 20, 2007

Spores of *Bacillus anthracis* are the infectious agent of anthrax. Current antibiotic treatments are limited due to resistance and patient age restrictions; thus, additional targets for therapeutic intervention are needed. One possible candidate is dihydrofolate reductase (DHFR), a biosynthetic enzyme necessary for anthrax pathogenicity. We determined the crystal structure of DHFR from *B. anthracis* (baDHFR) in complex with methotrexate (MTX; **1**) at 2.4 Å resolution. The structure reveals the crucial interactions required for MTX binding and a putative molecular basis for how baDHFR has natural resistance to trimethoprim (TMP; **2**). The structure also allows insights for designing selective baDHFR inhibitors that will have weak affinities for the human enzyme. Additionally, we have found that 5-nitro-6-methylamino-isocytosine (MANIC; **3**), which inhibits another *B. anthracis* folate synthesis enzyme, dihydropteroate synthase (DHPS), can also inhibit baDHFR. This provides a starting point for designing multi-target inhibitors that are less likely to induce drug resistance.

Introduction

Anthrax is a disease with a high mortality rate normally caused by the ingestion or inhalation of spores of the disease's etiological agent, the Gram-positive aerobic soil bacterium *Bacillus anthracis*. *B. anthracis* has received greater attention as of late because of its demonstrated use in bioterrorism.[1] Prevention of *B. anthracis* infection through vaccination and postexposure treatment with antibiotic regimes offer two lines of defense against anthrax. Indeed, a recent study on rhesus macaques has found that vaccination in concert with antibiotic treatment can significantly reduce the total time duration of antibiotic administration required to protect against inhalational anthrax.[2] However, current anthrax vaccines normally require regular administration of boosters over an 18 month period for maintaining immunity.[3,4] Prophylactic treatment of anthrax necessitates that antibiotics be administered to the patients prior to the manifestation of symptoms.[5] Unfortunately, some of these therapies have serious limitations due to resistance.[6,7] *B. anthracis* is naturally resistant to trimethoprim (TMP[a]; **2**),[8] sulfonamides, and some cephalosporins. The standard prophylaxis after anthrax exposure is the second-generation fluoroquinolone ciprofloxacin,[9] a topoisomerase inhibitor, which is not licensed for use in children. Further, the presence and continuous development of drug resistance requires the scientific community to continue development of new drug antimicrobial agents.[10]

B. anthracis dihydrofolate reductase (baDHFR) is a valid drug target because it is essential for the survival and pathogenesis of anthrax.[8,11] Nearly all prokaryotes must synthesize folate compounds de novo, starting with GTP and utilizing several different enzymes in a multistep pathway.[12,13] DHFR is required for the recycling of tetrahydrofolate (THF), a necessary cofactor used in several diverse biosynthetic pathways where one-carbon transfer reactions occur, such as in thymine and methionine synthesis.[14] It catalyzes the NADPH-dependent reduction of 7,8-dihydrofolate (DHF), producing 5,6,7,8-THF.[15] Loss of DHFR function via inhibition depletes THF pools, causing genomic and proteomic instability and, ultimately, cell death.[16] Thus, DHFRs from pathogenic bacterial species such as *B. anthracis* serve as attractive antimicrobial drug targets. Common DHFR inhibitors used in a clinical setting include TMP (a selective antibacterial), amethopterin or methotrexate (MTX; a chemotherapeutic against certain cancers and rheumatoid arthritis), and pyrimethamine (PYR; an antimalarial).[16−18] However, there are disadvantages to using each of these compounds as agents against anthrax. As stated earlier, *B. anthracis* is naturally resistant to TMP.[8] MTX binds potently to human DHFR,[16] excluding it from use as an antibiotic. PYR seems to be fairly selective for malarial DHFR.[19]

Two steps upstream of DHFR in the prokaryotic folate synthesis pathway is dihydropteroate synthase (DHPS), whose function is to catalyze the formation of dihydropteroate by condensing hydroxymethyl-7,8-dihydropteridine pyrophosphate with *para*-aminobenzoic acid (*p*-ABA). Recently, the structure of DHPS from *B. anthracis* (baDHPS) was solved in complex with several different compounds; most of these structures helped elucidate details of the enzyme mechanism.[20] However, one of the reported structures was baDHPS bound to 5-nitro-6-methylamino-isocytosine (MANIC; **3**), an inhibitor compound that targeted the pteridine ring binding site and not the *p*-ABA binding site, where sulfa drugs target. This is favorable due to sulfonamide resistance being discovered in many pathogenic bacterial species, especially against sulfamethoxazole (SMX).[21] A standard synergistic treatment for some urinary and respiratory tract infections and for pneumocystis pneumonia is the drug combination of SMX and TMP, which acts as a "sequential blockade" of the folate synthesis pathway.[17] A similar synergy treatment is used against malaria patients infected with *Plasmodium falciparum* and involves using sulfadoxin and PYR, although rapid resistance rates have been recently reported.[22,23]

† Coordinates for the baDHFR·MTX structure have been deposited in the Protein Data Bank under the accession number 2QK8.

* To whom correspondence should be addressed. Phone: (865) 974-4088. Fax: (865) 974-6306. E-mail: cdealwis@utk.edu.

‡ University of Tennessee.

§ University of Tennessee Health Sciences Center.

[a] Abbreviations: DHFR, dihydrofolate reductase; MTX, methotrexate; DHPS, dihydropteroate synthase; MANIC, 5-nitro-6-methyl aminoisocytosine; TMP, trimethoprim; SMX, sulfamethoxazole; PYR, pyrimethamine; *p*-ABA, *para*-aminobenzoic acid; IC_{50}, inhibitor concentration at 50% enzymic rate inhibition.

10.1021/jm070319v CCC: $37.00
Published on Web 08/14/2007

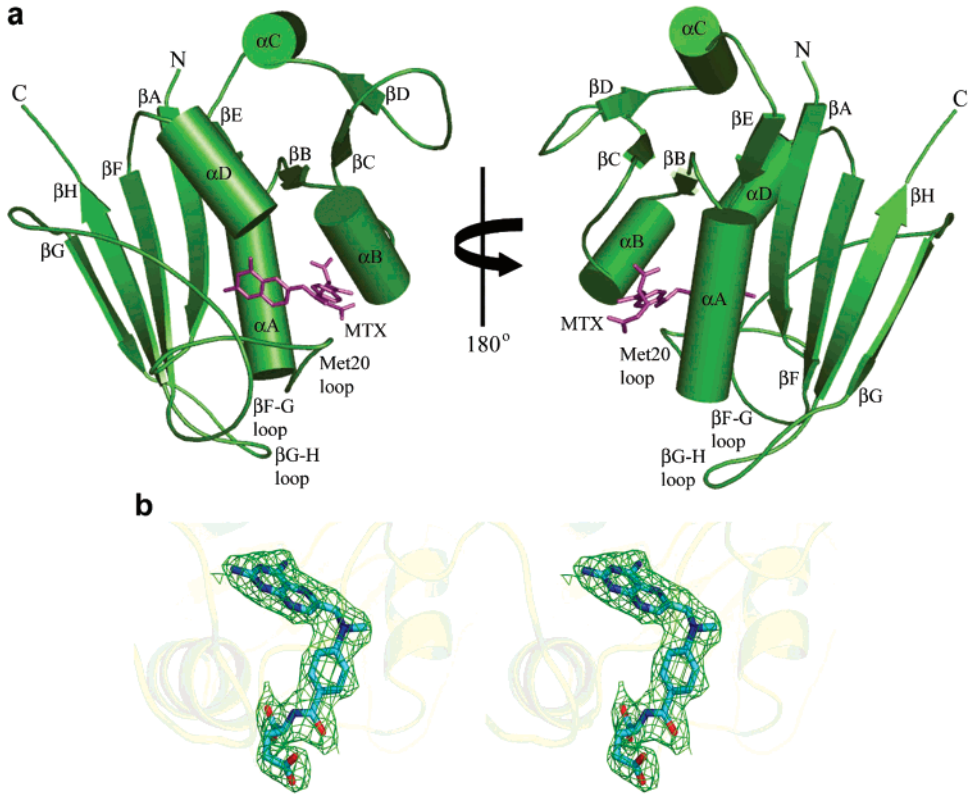

Figure 1. Crystal structure of baDHFR bound to MTX. (a) Anthrax DHFR adopts the canonical nucleotide-binding oxidoreductase fold,[5] with eight β strands and four flanking α-helices. Two views of the tertiary structure of baDHFR are shown, rotated 180° with respect to each other. In addition to MTX (magenta) and sequence termini, secondary structure elements have been labeled, including the important regulatory loops (Met20, βF-G, and βG-H). (b) Stereoview of $2F_o - F_c$ electron density contoured at 1σ about the MTX molecule.

So, the DHPS inhibitor MANIC (**3**), or a close analogue thereof, may also be a good lead candidate against other enzymes with pteridine binding pockets, like DHFR. This could prove to be advantageous because one could target multiple enzymes (i.e., DHPS and DHFR) in the same biosynthetic pathway of anthrax with the same drug, thus triggering sequential blockade with a single compound instead of a synergistic combination like TMP−SMX. A multi-target therapeutic approach has been suggested to be a proficient method for reducing the possibility of resistance;[24−26] perhaps this is an important consideration in terms of the development of mass prophylaxis against anthrax.

Here we report the crystal structure of DHFR from *B. anthracis* bound to the well-known anticancer and anti-inflammatory agent, methotrexate (MTX; **1**). Analysis of the baDHFR structure allows comparison to DHFRs from other pathogenic prokaryotic species as well as to hsDHFR. Molecular details of inhibitor binding provide a starting point for rational design of drug compounds against baDHFR. We discuss this in light of kinetic (for **3**) and modeling (for **3**; and two new diaminopyrimidines, Iclaprim (**4**) and **5** (AR-709)) data for three potential baDHFR inhibitory compounds.

Results and Discussion

We have determined the crystal structure of wild type baDHFR in complex with **1** using molecular replacement, and it has been refined to 2.4 Å resolution (Figure 1a). Our structure has been refined with an R_{free} of 27.4% with reasonable stereochemistry (Table 1). Over 99% of the main chain conformation lies within the allowed region of the Ramachandran plot. The $2F_o - F_c$ electron density map clearly defines **1** bound at the baDHFR active site (Figure 1b). Additionally, we determined the IC_{50} for **3** against baDHFR to be 104 μM (see Supporting Table 1 and Supporting Figure 1 for kinetic data).

Table 1. X-ray Crystallographic Statistics for the baDHFR·MTX Crystal

unit cell		
a, *b*, *c* (Å)	82.70, 41.24, 67.03	
β (deg)	119.2	
space group	*C*2	
	resolution range 58.0−2.2 Å	highest resolution shell 2.3−2.2 Å
total reflections	220 659	17 056
unique reflections	16 860	1302
completeness (%)	92.3	76.5
R_{symm} (%)[a]	9.6	34.2
I/σ	12.1	2.8
multiplicity	3.3	2.9
refinement resolution range 58.0−2.4 Å		
R_{work}/R_{free} (%)[b]	24.3/27.4	
no. of atoms		
protein	1346	
ligand	32	
solvent	47	
average B-factors (Å^2)		
protein	45.1	
ligand	27.6	
solvent	37.7	
deviations from ideality[c]		
bond lengths (Å)	0.017	
bond angles (deg)	1.90	

[a] $R_{symm} = \sum_{hkl} \sum_i \mathrm{II}_{i(hkl)} - I_{hkl}\mathrm{I}/\sum_{hkl} \sum_i I_{(hkl)}$. [b] R_{work} and $R_{free} = \sum||F_o| - |F_c||/\sum|F_o|$, where F_o and F_c are the observed and calculated structure factor amplitudes. For the calculation of R_{free}, 5% of the reflection data was randomly selected and omitted from refinement. [c] Values from the final refinement cycle in Refmac.[41]

General Features of baDHFR Sequence and Structure: Comparison to Other Species. baDHFR is a 19 kDa protein

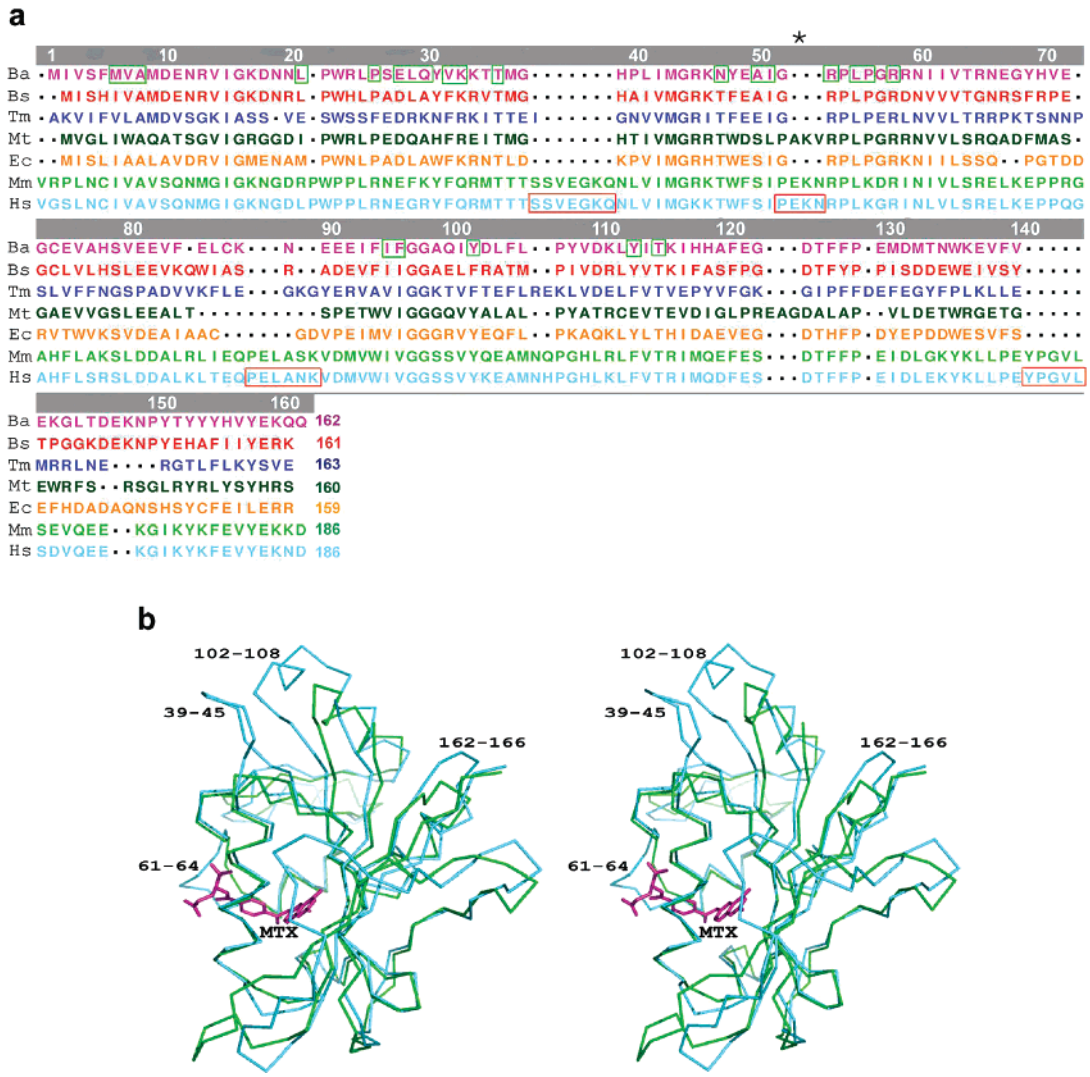

Figure 2. Three-dimensional structure-based sequence alignment and superposition of DHFR structures. (a) The alignment was performed using the baDHFR structure as the reference structure. It is in the following order: baDHFR (*Bacillus anthracis*), bsDHFR (*Bacillus stearothermophilus*), tmDHFR (*Thermatoga maritima*), mtDHFR (*Mycobacterium tuberculosis*), ecDHFR (*Escherichia coli*), mmDHFR (*Mus musculus*), and hsDHFR (*Homo sapiens*). The hsDHFR inserts (red boxes) and the baDHFR residues forming the MTX binding site (green boxes) have been indicated for clarity. The numbers shown above the sequence alignment correspond to the baDHFR sequence. (b) A stereoview of the superposition of baDHFR (green) and hsDHFR (cyan), both shown as Cα traces. The inserts are denoted using hsDHFR sequence numbering. The MTX (magenta) shown is from the baDHFR structure.

that shares 31.8% and 38.9% sequence identity with the human and *Escherichia coli* enzymes, respectively (Figure 2a; numbering corresponds to the baDHFR sequence unless specified). A striking difference between the human and the baDHFR sequences occurs due to loop insertions between positions 39−45, 61−64, 103−105, and 162−166, corresponding to the human DHFR (hsDHFR) sequence. The first two insertions in hsDHFR are involved in drug interactions absent in baDHFR; these differences can be exploited for designing selective therapies. Although the tertiary structure of baDHFR, consisting of the canonical eight-stranded twisted β-sheet fold, is extremely conserved between species (Figures 1a and 2b), there are significant sequence differences at the inhibitor binding site (Figure 2a) making it necessary to have the baDHFR structure as a template for knowledge-based drug design. To this end, we determined the crystal structure of wild type baDHFR in complex with **1**. MTX (**1**), an antifolate and one of the first chemotherapeutics discovered,[16] is a tight-binding DHFR inhibitor that shows little species selectivity but is a powerful drug against several forms of cancer and as an immunosuppressant against rheumatoid arthritis.[12] Elucidation of its binding conformation and interactions in the present structure provide a template for rational drug design.

Comparison of baDHFR to DHFRs from Two Other Prokaryotic Pathogens. The structures of *Lactobacillus casei* DHFR (lcDHFR)[27] and *Mycobacterium tuberculosis* DHFR (mtDHFR)[28] are very similar to the baDHFR structure (Supporting Figure 2a), and they share 36.6% and 35.3% sequence identity with the *Bacillus* enzyme, respectively. One of the major conformational differences between all three structures occurs within a turn region between α-helix B and β-strand C, at Gly 52. The equivalent residue to Gly52 in baDHFR is proline in both lcDHFR and mtDHFR (Supporting Figure 2b). This residue is very near the active site and is discussed below. A loop near the C-terminus (called the βG-H loop; residues 142−153 of baDHFR) adopts different conformations among the three species, with the baDHFR βG-H loop packing nearer to the C-terminal end of the active site loop (called the Met20 loop; residues 11−25) than the same loop in lcDHFR and mtDHFR.

The baDHFR Binding Site for MTX: Comparison to Human DHFR. The pteridine ring of the MTX molecule binds at the active site of baDHFR with its N1 and the NA2 atoms

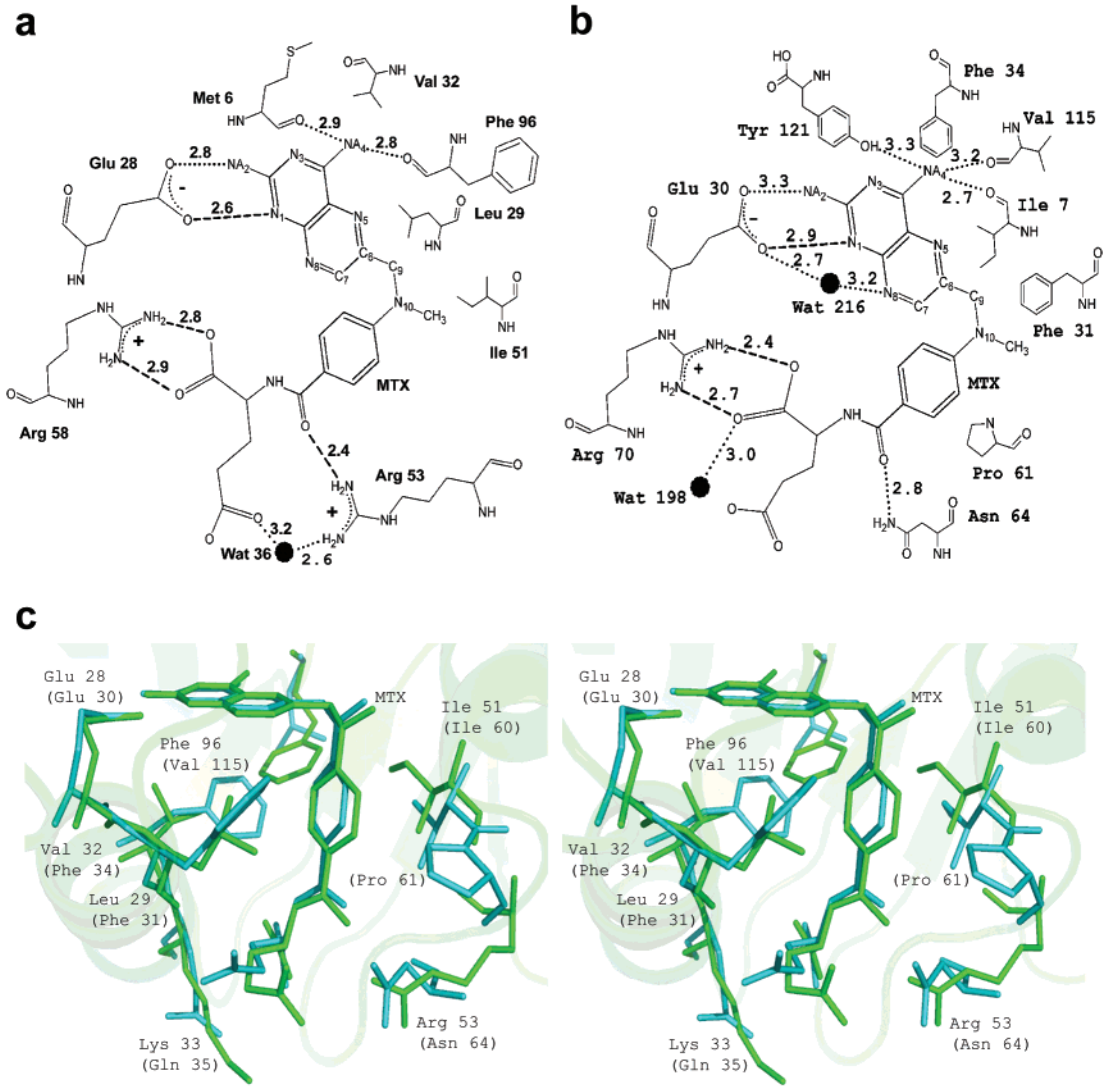

Figure 3. baDHFR-MTX binding site and comparison to hsDHFR-MTX binding. (a) A schematic representation of baDHFR−MTX interactions (dotted lines depict hydrogen bonds, and dashed lines indicate ion-pair interactions). (b) For comparison, a schematic of the hsDHFR−MTX interactions is shown. (c) A stereoview of the MTX binding site, with key residues shown from baDHFR (green) and hsDHFR (cyan) that are involved in ligand binding. The corresponding MTX molecules bound to the two DHFRs are drawn in the respective colors.

interacting with the carboxyl group of the catalytic Glu 28 (Figure 3a). The MTX N1 atom, which was shown to be protonated (and, thus, charged) in a recent neutron diffraction study of the *E. coli* DHFR complex,[29] forms a salt-bridge with the Oϵ2 of Glu 28, while the N2 atom hydrogen bonds to Oϵ1. Also, the N4 atom of the pteridine ring forms a bifurcated hydrogen bond to the carbonyl oxygens of the Met 6 and Phe 96 residues.

MTX (**1**) inhibits baDHFR with a 2-fold improvement over hsDHFR.[8] However, comparison of the MTX modes of binding between baDHFR and hsDHFR reveals striking similarities. The pteridine ring binds both baDHFR and hsDHFR almost identically, except there is a complementary Val to Phe substitution at positions 32 and 96 (baDHFR numbering, Figure 2a). A structural consequence of this substitution is that the Phe in the human enzyme makes a more favorable stacking interaction with the pteridine ring as compared to baDHFR (Figure 3b−d). The benzyl ring of the *p*ABA-glutamate (*p*-ABA-Glu) tail moiety of **1** binds at a hydrophobic pocket packed between Leu 29 and Ile 51. In hsDHFR, the Leu residue is substituted by an aromatic Phe resulting in an edge-on stacking interaction with the benzyl moiety, and an additional van der Waals interaction is made by Pro 61, which is the first residue of the aforementioned loop insertion (Figures 2a,b, 3b−d). Interestingly, both the bacterial pathogens lcDHFR and mtDHFR, unlike baDHFR, also have proline at this position. In both baDHFR and hsDHFR, the *p*-ABA-Glu tail of **1** is stabilized mainly by similar hydrogen bonds and ion-pair interactions. However, the Arg 53 to Asn 64 and Lys 33 to Gln 35 (baDHFR to hsDHFR) substitutions result in a conformational change at the carboxylate side chain of the *p*-ABA-Glu tail of **1** (Figure 3b−d). In baDHFR, the guanidinium group of Arg 53 forms bifurcated salt-bridges with the carbonyl oxygen and the side chain of the *p*-ABA-Glu tail, while in hsDHFR, Asn 64 hydrogen bonds with the carbonyl oxygen of the *p*-ABA-Glu tail but is too far to interact with its side-chain carboxylate. Lysine 33 of baDHFR forms an ion-pair interaction with the side-chain carboxylate of the *p*-ABA-Glu tail, an interaction that is missing in hsDHFR due to the substitution of Gln. Interestingly, the number of hydrogen bonds and van der Waals contacts made by baDHFR and hsDHFR with MTX is almost identical. However, baDHFR makes 50% more ion-pair interactions than hsDHFR, possibly explaining the enhanced inhibition by MTX of the former.[8]

A Mechanism for the Natural Resistance of *Bacillus anthracis* to TMP. TMP (**2**) is an important antibiotic used synergistically with the sulfonamide class of compounds for

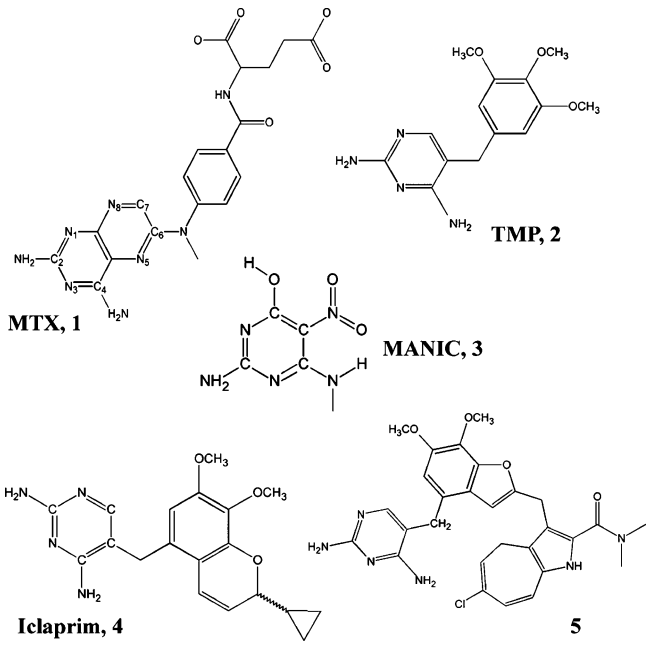

Figure 4. Chemical structures of important DHFR inhibitory compounds.

many types of infections[21,30] (Figure 4 and Supporting Table 1). However, recent structure−activity relationship (SAR) studies have reported that **2** inhibits *Bacillus* DHFRs relatively poorly ($IC_{50} = \sim 77\ \mu M$).[8] With the availability of the baDHFR structure, it is possible to investigate the molecular basis of TMP resistance. In *Staphylococcus aureus*, a mutation of Phe 98 to Tyr (Tyr 102 in baDHFR) and, in *Streptococcus pneumoniae*, a mutation of Ile 100 to Leu (Ile 95 in baDHFR) have been reported to confer resistance to TMP inhibition.[31,32] Modeling studies (where TMP was manually docked into the baDHFR active site and then the complex was energy minimized) reveal that Tyr 102 and Ile 95 are distant from the putative TMP binding site in baDHFR (Figure 5a); however, it has been proposed that distal residues play a role in DHFR catalytic function.[33] The substitution of Ile (the residue found in the other prokaryotic DHFRs shown in Figure 2a) to Phe at position 96 in baDHFR could be the crucial mutation for the loss of inhibition, as it sterically interferes with the benzyl linkage bridging the diaminopyrimidine and the trimethoxyphenyl rings of **2** and makes close contacts with the trimethoxyphenyl ring itself (Figure 5a). In silico, when we mutate baDHFR Phe 96 to an Ile and perform energy minimization, we observe no steric clashes, further confirming that Phe 96 is crucial to TMP resistance. However, we cannot rule out the influence of other residues on TMP resistance.

Inhibition of baDHFR by the Small DHPS Inhibitor, MANIC. MANIC (**3**; Figure 4) was first synthesized as a member of a new class of DHPS inhibitors that specifically would bind in the pterin ring pocket of the active site and interfere with dihydropterin pyrophosphate substrate binding. This was novel in that these 5-nitro-isocytosine compounds were designed to not compete with the other substrate, *p*-ABA, at its binding site on DHPS, where sulfonamide drugs traditionally bind.[34] In this way, they would evade emerging resistance in pathogenic bacteria. The IC_{50} for **3** against *E. coli* DHPS was determined to be 2.8 μM.[34] More recently, the crystal structure of *B. anthracis* DHPS has been solved with **3** bound at the active site.[20] Indeed, it binds at the pterin substrate binding pocket. We were interested if **3** could also inhibit baDHFR and act as a multi-target inhibitor that can inhibit two enzymes in the same biosynthetic pathway. MANIC inhibits baDHFR with an IC_{50} of 104 μM (see Supporting Table 1 and Supporting Figure 1), higher than the reported IC_{50} against *E. coli* DHPS[34] but inhibitory nonetheless. We postulate that **3** competes with the pterin ring of the DHF substrate for binding to baDHFR. Indeed, preliminary kinetic studies indicate that **3** is a competitive inhibitor. MANIC (**3**) is quite small (MW = 185 Da) relative to the common antifolate and sulfonamide drugs (MW > 400 Da). We can use **3** as a fragment[35] to build compounds that are more potent against baDHFR, possibly while still maintaining or even enhancing binding to DHPS. The advantage of this validated approach is that it is much harder for the pathogen to develop resistance when a drug has activity against multiple targets.[26]

We have modeled **3** into the baDHFR active site (Figure 5b). MANIC (**3**) can potentially form four hydrogen bonds to baDHFR, two of which are the conserved electrostatic interactions between the Glu 28 carboxylate and the N1 and N2 atoms of the pyrimidine ring of the inhibitor. The third and fourth are interactions between the hydroxyl of **3** and the carbonyl oxygens of Met 6 and Phe 96. Although the methyl group on **3** can freely rotate, it has been modeled as planar as observed in the baDHPS crystal structure.[20] The methyl is seated within a hydrophobic cleft composed of the side chains of Leu 21 and Leu 29 and the Cβ of Glu 28. As modeled, baDHFR makes no interactions with the nitrate group of **3**. The Nδ2 atom of Asn 47 is 4 Å away from one of the oxygens of the nitrate group, so by extending this group on **3** closer to Asn 47 one could optimize interactions to baDHFR and improve affinity.

Toward the Rational Design of Selective baDHFR Inhibitor Compounds. A viable therapeutic agent against anthrax will have to be selective for the pathogen while binding poorly to its human host. Though **1** is a potent inhibitor against baDHFR ($IC_{50} = 15-25$ nM[8,11]), it is unselective and is a potent inhibitor of hsDHFR, rendering it ineffective as a specific drug against anthrax. The lack of selectivity of **1** and the natural resistance of **2** for baDHFR require the development of new classes of inhibitors. Modified pteridine and pyrimidine analogues designed with the aid of the knowledge-based approach will enable the synthesis of highly potent selective drugs. Furthermore, the sequence deviations between baDHFR and hsDHFR at the inhibitor binding site strongly suggest that this can be exploited for designing selective drugs. For example, a structural comparison of the baDHFR and the hsDHFR shows that the following sequence substitutions—Met 6 to Ile 7, Phe 96 to Val 115, Leu 29 to Phe 31, Val 32 to Phe 34, Lys 33 to Gln 35, Ala 50 to Ser 59, Asn 47 to Thr 56, and the Pro 61 insert in the human enzyme—occur at the inhibitor binding site (Figures 2a, 5c). Specifically, the Leu 29 to Phe 31 substitution and the Pro 61 insert can be exploited for providing selectivity against hsDHFR; the bulky Phe and Pro residues form the hydrophobic pocket involved in binding the benzyl moieties (Figure 5c) of inhibitor compounds. By substituting the benzyl moiety with more bulky groups, steric constraints will be imposed and obstruction of hsDHFR binding can be achieved. In fact, it has been recently reported that two new diaminopyrimidine analogues with such structural characteristics, Iclaprim (**4**, formally AR-100) and **5** (both compounds developed by Arpida Ltd., Switzerland; Figure 4), can selectively inhibit DHFRs from certain pathogenic bacterial species, including a TMP-resistant *Staphylococcus aureus* (MRSA) strain, over the human enzyme.[13,36−38]

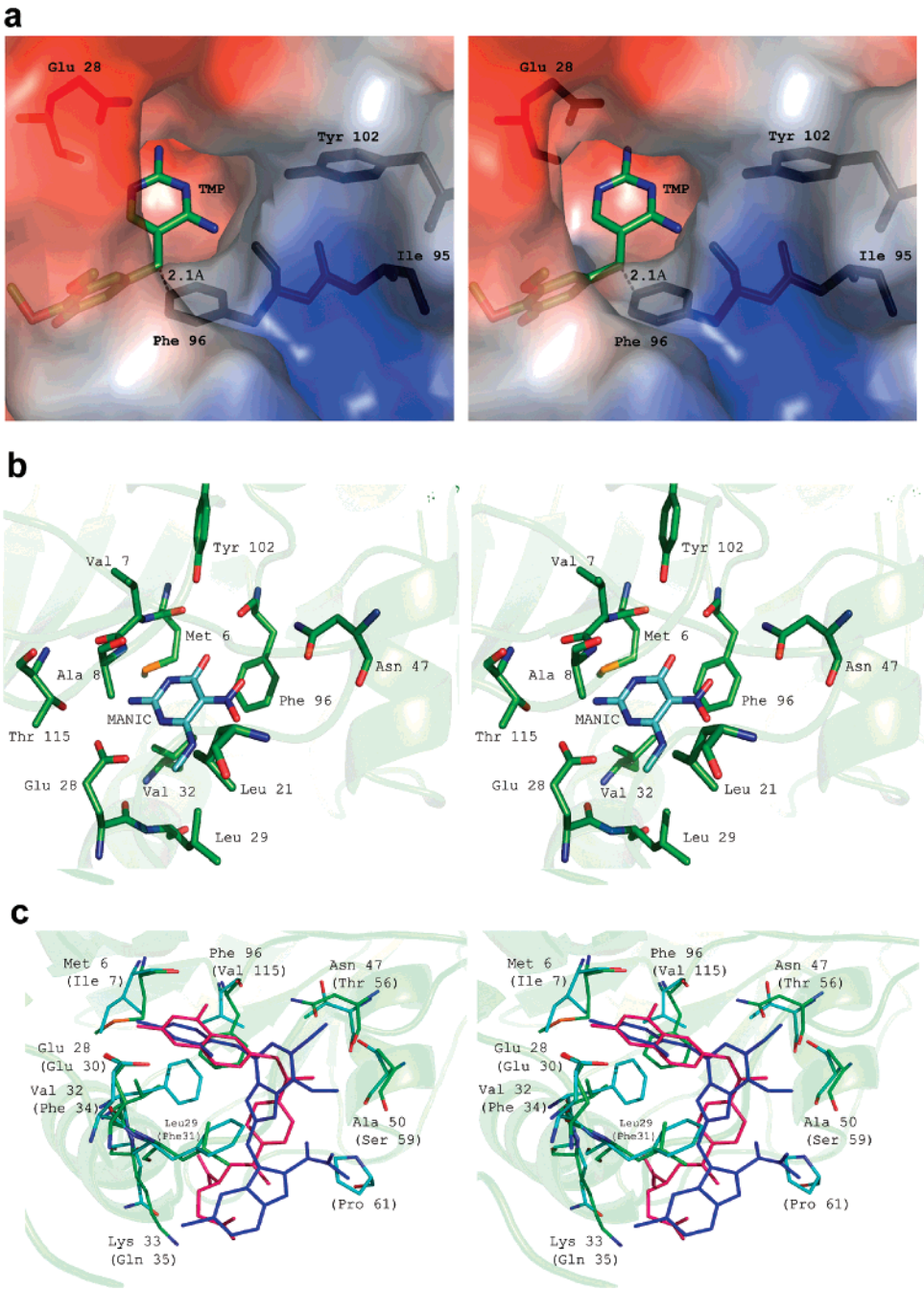

Figure 5. Characterization and comparison of TMP, MANIC, and **5** binding to baDHFR. Ligands were manually modeled into the substrate binding sites of baDHFR or hsDHFR using MTX as a template to guide the docking. The complexes were then refined using energy minimization. (a) Stereoview of trimethoprim (oxygen: red, carbon: green, nitrogen: blue) modeled into the baDHFR active site depicted as an electrostatic surface (negative charge: red, positive charge: blue, apolar: white), (b) Stereoview of MANIC (colored by atom; blue: nitrogen, red: oxygen, yellow: carbon), modeled into the baDHFR (green) active site. (c) Stereoview of the residues that deviate between baDHFR (green) and hsDHFR (cyan) at the inhibitor binding site. For demonstrating how to exploit the sequence deviation between baDHFR and hsDHFR, a recently described diaminopyrimidine compound (**5**, dark blue) that is highly selective against DHFRs from pathogenic bacterial species over hsDHFR has been modeled into the baDHFR and hsDHFR active sites. Note the clash of this compound with Pro 61 from hsDHFR. For reference, MTX (magenta) from our baDHFR structure has been superposed.

Compound **4** possesses broad-spectrum activity against DHFRs from Gram-positive and -negative pathogens, does not induce resistance among TMP-sensitive or insensitive *S. aureus* strains, and is currently in Phase III clinical trials as an intravenous therapy against complicated skin infections.[13,26] Compound **5** is in the preclinical stage but has shown broad-spectrum activity against multidrug-resistant pathogens responsible for respiratory tract infections.[13,38] Both of these compounds inhibit hsDHFR poorly (Supporting Table 1), with IC_{50} values of >300 μM. To investigate if these compounds can selectively bind baDHFR over hsDHFR, we conducted docking studies using our baDHFR crystal structure and an hsDHFR crystal structure (Figure 5c and Supporting Figure 3). Like **3**, the diaminopyrimidine rings of both of these compounds form conserved hydrogen bonds with key active site residues such as Glu 28 (Glu 30 for hsDHFR) (Figure 5c and Supporting Figure 3). However, the pyran and dimethoxyphenyl rings of **4** sterically clash with Phe 31, Phe 34, and Pro 61 of hsDHFR, clashes which are not observed with baDHFR due to the substitution of smaller side chains Leu 29, Val 32, and Gly 52,

respectively (Supporting Figure 3). Interestingly, the branched group of the benzopyrene ring of **5** will clash with Pro 61 of hsDHFR, while it should bind baDHFR without steric clashes (Figure 5c). The aforementioned multiple sequence substitutions clearly offer the opportunity to design selective inhibitors of baDHFR.

The three-dimensional structure of baDHFR reveals how drug molecules bind at the active site and provides a molecular basis for explaining existing SAR data, including its natural resistance to the commonly used antibacterial agent TMP. Studies with the small molecule MANIC which inhibits baDHPS and baDHFR, two members of the folate biosynthetic pathway, provides a useful starting point for the development of multi-target inhibitors that will be less prone to inactivation by a pathogen's resistance mechanisms. Our structure provides an accurate pharmacophore for designing new potent species-specific inhibitors against anthrax using the rational approach.

Experimental Section

Expression, Purification, and Crystallization of baDHFR. The cDNA was cloned into the Champion pET-Sumo vector (Invitrogen) and then transformed into chemically competent BL21(DE3) *E. coli* cells (Novagen-EMD Biosciences) for inducible protein expression. The overexpressed protein was purified using immobilized Nickel affinity (Ni-NTA; Qiagen) and weak anion exchange chromatography (DEAE2; Bio-Rad). Solid MTX (Sigma Aldrich) was added at 10× molar excess to the protein when the protein was at a relatively dilute concentration (~1 mg/mL). The baDHFR/MTX complex was crystallized at 4 °C at a concentration of 30 mg/mL using the hanging drop vapor diffusion method. The crystallization condition was 0.2 M $CaCl_2$ and 20% (w/v) PEG 3350.

X-ray Data Collection, Structure Solution, and Refinement. Synchrotron X-ray diffraction data were collected at the Advanced Photon Source (APS) on the BioCARS beamline 14-BM-C using an X-ray wavelength of 0.9 Å. The structure was determined by the molecular replacement method, as implemented in the program PHASER,[39] using the *Bacillus stearothermophilus* DHFR coordinates (PDB ID: 1ZDR) as the search model. Refinement was interspersed with model building using CNS,[40] REFMAC,[41] O,[42] and Coot.[43] The 3D structure-based sequence alignment (Figure 1a) was performed using MOE.[44] Models of ligands **2**−**5** were manually docked into the baDHFR or hsDHFR substrate binding sites. These docked models (protein−ligand complex) were then energy minimized using CNS and analyzed with O and Coot. Figures were generated using PyMol[45] and Chemsketch.[46]

Inhibition Kinetics. Steady-state reaction rates were measured for baDHFR activity in the absence (uninhibited rate) and presence of the MANIC (**3**) compound. MANIC was synthesized as reported in ref 20. Activity was measured as a change in absorbance over time at a wavelength of 340 nm (A_{340}), so as to monitor the disappearance of NADPH. The reaction buffer consisted of 50 mM $KHPO_4/K_2HPO_4$ (pH 7.1), 10 mM β-mercaptoethanol, and 1 mM K_2EDTA. The concentrations of substrate (DHF) and cofactor (NADPH) were kept constant for the experiment at 125 μM and 12.5 μM, respectively. The concentration of baDHFR used in the experiment (50 nM) was determined by its absorbance at 280 nm using a theoretically derived ϵ of 27 390 M^{-1} cm^{-1}. After incubation of the enzyme with **3** and NADPH for 2 min, the reaction was initiated with the addition of DHF and the A_{340} was plotted over the course of 1.5 min. Six different concentrations of **3** were utilized in the assays to determine the IC_{50}. All measurements that were used to calculate the IC_{50} of **3** against baDHFR were performed in triplicate or quadruplicate. The incubations and reactions were performed at room temperature.

Acknowledgment. We acknowledge the BioCARS staff at the APS for assistance in X-ray data collection. We gratefully acknowledge Drs. Esther and William Barrow and Dr. Andrew Mesacar for providing baDHFR cDNA. We appreciate Dr. Elizabeth Howell for critical reading of the manuscript, and Dr. Sanath Wijerathna for useful discussion. B.B. and H.X. were partially funded by a DOE LDRD award 20070131ER under subcontract 48676-001-07 to the University of Tennessee. The authors declare that they have no competing financial interests.

Supporting Information Available: A table of kinetic data, a graph showing **3**'s inhibition of baDHFR used to determine the IC_{50}, a stereo figure of superposed DHFRs from pathogenic bacterial species, and a stereo figure of **4** modeled into the baDHFR and hsDHFR active sites are provided. This material is available free of charge via the Internet at http://pubs.acs.org.

References

(1) Inglesby, T. V.; O'Toole, T.; Henderson, D. A.; Bartlett, J. G.; Ascher, M. S.; et al. Anthrax as a biological weapon, 2002: updated recommendations for management. *J. Am. Med. Assoc.* **2002**, *287*, 2236- 2252.
(2) Vietri, N. J.; Purcell, B. K.; Lawler, J. V.; Leffel, E. K.; Rico, P.; et al. Short-course postexposure antibiotic prophylaxis combined with vaccination protects against experimental inhalational anthrax. *Proc. Natl. Acad. Sci. U.S.A.* **2006**, *103*, 7813−7816.
(3) Swartz, M. N. Recognition and management of anthrax−an update. *N. Engl. J. Med.* **2001**, *345*, 1621−1626.
(4) Spencer, R. C. *Bacillus anthracis*. *J. Clin. Pathol.* **2003**, *56*, 182−187.
(5) Coker, P. R.; Smith, K. L.; Hugh-Jones, M. E. Antimicrobial susceptibilities of diverse *Bacillus anthracis* isolates. *Antimicrob. Agents Chemother.* **2002**, *46*, 3843−3845.
(6) Doganay, M.; Aydin, N. Antimicrobial susceptibility of *Bacillus anthracis*. *Scand. J. Infect. Dis.* **1991**, *23*, 333−335.
(7) Inglesby, T. V.; Henderson, D. A.; Bartlett, J. G.; Ascher, M. S.; Eitzen, E.; et al. Anthrax as a biological weapon: medical and public health management. Working Group on Civilian Biodefense. *J. Am. Med. Assoc.* **1999**, *281*, 1735−1745.
(8) Barrow, E. W.; Bourne, P. C.; Barrow, W. W. Functional cloning of *Bacillus anthracis* dihydrofolate reductase and confirmation of natural resistance to trimethoprim. *Antimicrob. Agents Chemother.* **2004**, *48*, 4643−4649.
(9) Grady, R. W. Systemic quinolone antibiotics in children: a review of the use and safety. *Expert Opin. Drug Saf.* **2005**, *4*, 623−630.
(10) Friedlander, A. M. Tackling anthrax. *Nature* **2001**, *414*, 160−161.
(11) Joska, T. M.; Anderson, A. C. Structure-activity relationships of *Bacillus cereus* and *Bacillus anthracis* dihydrofolate reductase: toward the identification of new potent drug leads. *Antimicrob. Agents Chemother.* **2006**, *50*, 3435−3443.
(12) Hitchings, G. H., Jr. Nobel lecture in physiology or medicine−1988. Selective inhibitors of dihydrofolate reductase. *In Vitro Cell Dev. Biol.* **1989**, *25*, 303−310.
(13) Hawser, S.; Lociuro, S.; Islam, K. Dihydrofolate reductase inhibitors as antibacterial agents. *Biochem. Pharmacol.* **2006**, *71*, 941−948.
(14) Huennekens, F. M. In search of dihydrofolate reductase. *Protein Sci.* **1996**, *5*, 1201−1208.
(15) Benkovic, S. J. On the mechanism of action of folate- and biopterin-requiring enzymes. *Annu. Rev. Biochem.* **1980**, *49*, 227−251.
(16) Huennekens, F. M. The methotrexate story: a paradigm for development of cancer chemotherapeutic agents. *Adv. Enzyme Regul.* **1994**, *34*, 397−419.
(17) Katzung, B.; Trevor, A. *Basic & Clinical Pharmacology*; 9th ed.; McGraw-Hill: New York, 2004.
(18) Hekmat-Nejad, M.; Rathod, P. K. *Plasmodium falciparum:* kinetic interactions of WR99210 with pyrimethamine-sensitive and pyrimethamine-resistant dihydrofolate reductase. *Exp. Parasitol.* **1997**, *87*, 222−228.
(19) Kongsaeree, P.; Khongsuk, P.; Leartsakulpanich, U.; Chitnumsub, P.; Tarnchompoo, B.; et al. Crystal structure of dihydrofolate reductase from *Plasmodium vivax*: pyrimethamine displacement linked with mutation-induced resistance. *Proc. Natl. Acad. Sci. U.S.A.* **2005**, *102*, 13046−13051.
(20) Babaoglu, K.; Qi, J.; Lee, R. E.; White, S. W. Crystal structure of 7,8-dihydropteroate synthase from *Bacillus anthracis*: mechanism and novel inhibitor design. *Structure* **2004**, *12*, 1705−1717.
(21) Huovinen, P.; Sundstrom, L.; Swedberg, G.; Skold, O. Trimethoprim and sulfonamide resistance. *Antimicrob. Agents Chemother.* **1995**, *39*, 279−289.
(22) Sibley, C. H.; Hyde, J. E.; Sims, P. F.; Plowe, C. V.; Kublin, J. G.; et al. Pyrimethamine-sulfadoxine resistance in *Plasmodium falciparum*: what next? *Trends Parasitol.* **2001**, *17*, 582−588.
(23) Roper, C.; Pearce, R.; Nair, S.; Sharp, B.; Nosten, F.; et al. Intercontinental spread of pyrimethamine-resistant malaria. *Science* **2004**, *305*, 1124.

(24) Silver, L. L.; Bostian, K. A. Discovery and development of new antibiotics: the problem of antibiotic resistance. *Antimicrob. Agents Chemother.* **1993**, *37*, 377−383.
(25) Spratt, B. G. Resistance to antibiotics mediated by target alterations. *Science* **1994**, *264*, 388−393.
(26) Silver, L. L. Multi-targeting by monotherapeutic antibacterials. *Nat. Rev. Drug Discov.* **2007**, *6*, 41−55.
(27) Bolin, J.; Filman, D.; Matthews, D.; Hamlin, R.; Kraut, J. Crystal structures of *Escherichia coli* and *Lactobacillus casei* dihydrofolate reductase refined at 1.7 Å resolution. I. General features and binding of methotrexate. *J. Biol. Chem.* **1982**, *257*, 13650.
(28) Li, R.; Sirawaraporn, R.; Chitnumsub, P.; Sirawaraporn, W.; Wooden, J.; et al. Three-dimensional structure of *M. tuberculosis* Dihydrofolate Reductase reveals opportunities for the design of novel tuberculosis drugs. *J. Mol. Biol.* **2000**, *295*, 307−323.
(29) Bennett, B. C.; Langan, P.; Coates, L.; Mustyakimov, M.; Schoenborn, B.; et al. Neutron diffraction studies of *Escherichia coli* Dihydrofolate Reductase bound to the anticancer drug Methotrexate. *Proc. Natl. Acad. Sci. U.S.A.* **2006**, *103*, 18493−18498.
(30) Kasanen, A.; Sunqvist, H. Trimethoprim alone in the treatment of urinary tract infections: eight years of experience in Finland. *Rev. Infect. Dis.* **1982**, *4*, 358−365.
(31) Dale, G. E.; Broger, C.; D'Arcy, A.; Hartman, P. G.; DeHoogt, R.; et al. A single amino acid substitution in *Staphylococcus aureus* dihydrofolate reductase determines trimethoprim resistance. *J. Mol. Biol.* **1997**, *266*, 23−30.
(32) Adrian, P. V.; Klugman, K. P. Mutations in the dihydrofolate reductase gene of trimethoprim-resistant isolates of *Streptococcus pneumoniae*. *Antimicrob. Agents Chemother.* **1997**, *41*, 2406−2413.
(33) Agarwal, P. K.; Billeter, S. R.; Rajagopalan, P. T.; Benkovic, S. J.; Hammes-Schiffer, S. Network of coupled promoting motions in enzyme catalysis. *Proc. Natl. Acad. Sci. U.S.A.* **2002**, *99*, 2794−2799.
(34) Lever, O. W., Jr.; Bell, L. N.; McGuire, H. M.; Ferone, R. Monocyclic pteridine analogues. Inhibition of *Escherichia coli* dihydropteroate synthase by 6-amino-5-nitrosoisocytosines. *J. Med. Chem.* **1985**, *28*, 1870−1874.
(35) Rees, D. C.; Congreve, M.; Murray, C. W.; Carr, R. Fragment-based lead discovery. *Nat. Rev. Drug Discov.* **2004**, *3*, 660−672.
(36) Hartman, P. G.; Kompis, I.; Jaeger, J.; Mukhija, S.; Islam, K. AR-100, a novel diaminopyrimidine, can overcome TMP-resistance in staphylococci and streptococci. *ICAAC: Interscience Conference on Antimicrobial Agents and Chemotherapy*; American Society of Microbiology: Washington, DC, 2002.
(37) Schneider, P.; Hawser, S.; Islam, K. Iclaprim, a novel diaminopyrimidine with potent activity on trimethoprim sensitive and resistant bacteria. *Bioorg. Med. Chem. Lett.* **2003**, *13*, 4217−4221.
(38) Hawser, S.; Bihr, M.; Weiss, L.; Islam, K.; Lociuro, S. AR-709, A Novel Diaminopyrimidine Compound: Resistance Studies in Trimethoprim-Sensitive and -Resistant Bacteria. *ICAAC − Interscience Conference on Antimicrobial Agents in Chemotherapy*, 2006.
(39) McCoy, A. J.; Grosse-Kunstleve, R. W.; Storoni, L. C.; Read, R. J. Likelihood-enhanced fast translation functions. *Acta Crystallogr., Sect. D: Biol. Crystallogr.* **2005**, *61*, 458−464.
(40) Brunger, A. T.; Adams, P. D.; Clore, G. M.; DeLano, W. L.; Gros, P.; et al. Crystallography & NMR system: A new software suite for macromolecular structure determination. *Acta Crystallogr., Sect. D: Biol. Crystallogr.* **1998**, *54* (Pt 5), 905−921.
(41) Murshudov, G.; Vagin, A.; Dodson, E. Refinement of structures by the maximum-likelihood method. *Acta Crystallogr., Sect. D: Biol. Crystallogr.* **1997**, *D53*, 240−255.
(42) Jones, T. A.; Zou, J. Y.; Cowman, S. W.; Kjeldgaard, M. Improved methods for building protein models in electron density maps and the location of errors in these models. *Acta Crystallogr., Sect. A* **1991**, *47*, 110−116.
(43) Emsley, P.; Cowtan, K. Coot: model-building tools for molecular graphics. *Acta Crystallogr., Sect. D: Biol. Crystallogr.* **2004**, *60*, 2126−2132.
(44) CCG *Molecular Operating Environment*; Chemical Computing Group Inc.
(45) DeLano, W. L. *The PyMOL User's Manual*; DeLano Scientific: San Carlos, CA, 2002.
(46) Advanced Chemistry Development, I. *Chemsketch 10.0*; 10.0 ed.; Advanced Chemistry Development, Inc.: Toronto.

JM070319V